National Transportation Safety Board

Office of Research and Engineering

Washington, DC 20594

RRD22LR001

MATERIALS LABORATORY

Specialist's Factual Report - Supplemental 22-032C

March 13, 2023

(This page intentionally left blank)

MARCH 13, 2023 1
A. ACCIDENT INFORMATION 2
B. COMPONENTS EXAMINED 2
C. EXAMINATION PARTICIPANTS 2
D. DETAILS OF THE EXAMINATION 2

A. ACCIDENT INFORMATION

Location: Arlington, Virginia
Date: October 12, 2021
Time: 4:50pm eastern daylight time
Vehicle: WMATA Metro Blue Line
Investigator: Joe Gordon, RPH-10

B. COMPONENTS EXAMINED

Sections of railcar axle

C. EXAMINATION PARTICIPANTS

Specialist Erik Mueller, Ph.D., P.E.
Office of Research and Engineering – Materials Laboratory Division
NTSB

D. DETAILS OF THE EXAMINATION

This report is an addendum to the *22-032 Materials Laboratory Factual Report*. This report details an additional examination of the accident wheelset axle that involved destructive testing.

Figure 1 shows the three axles as received. The axle depicted on the bottom, axle 001352, was the axle of the derailed wheelset from the accident. The wheel seats of the accident axle had been partially ground to facilitate dimensional measurements by the Washington Metropolitan Area Transit Authority (WMATA) before receipt by the NTSB.

Figure 2 shows the wheel seat and the bearing journal of the left, or gearbox, side of the accident axle. The right-side wheel seat and bearing surfaces are shown in Figure 3 and Figure 4. The wheel seats of the accident axle were examined to inspect for indications of erosion and possible movement. After cleaning with a scouring pad and soapy water, followed by isopropyl alcohol, underlying features were observed consistent with bands of fretting wear and entrained particle damage. Localized plastic deformation and microscopic pit-like features were observed on the wheel seat surfaces. Prior to cleaning, the inboard portions of the wheel seat surfaces exhibited enough oxidation to obscure the underlying surface features—these characteristics were consistent with fretting wear.

This band of fretting wear was visible to the naked eye, located on the right-side wheel seat of the axle approximately 0.75 inches in width, as shown in Figure 4. Outboard of the visual fretting wear band was an area of thin erratic gouges, oriented

parallel to the axle direction. A closer examination of this region found this was consistent with entrained particles that had been ground into the axle during the removal (press-off) of the right-side wheel.

The right axle wheel seat area was sectioned parallel to the longitudinal direction, as highlighted in Figure 4. Figure 5 shows a montage of the surface of the excised portion of the axle. The section had been cleaned in an ultrasonic bath using acetone.

WMATA had categorized certain circumferential areas of the inboard wheel seat surface as Areas 'A,' 'B,' and 'C,' based on the apparent thickness of the surface oxidation (rust). The distances of each of these areas were annotated in Figure 5. Area A was approximately 0.29 inches in width from the inboard groove, B was a further 0.18 inches, and the width of C was 0.28 inches outboard of Area B. The width of the outboard band of fretting wear was measured as 0.41 inches, with the most severe damage being the inboard-most 0.27 inches. This band of fretting wear was located 1.30 inches from the inboard groove of the wheel seat.

Figure 6 shows a closer view of the most severe area of fretting wear damage. This region exhibited parallel wavy/linear features, oriented perpendicular to the longitudinal direction of the axle. The bands exhibited a brownish-maroon color, consistent with localized oxidation (rust) on the surface. Figure 7 shows a closer view of this region, demonstrating the folds and localized deformation on the surface.

Figures 8 and 9 show differential optical shadowing and false color overlaying of the image geometry, respectively, to illustrate and amplify the morphology of the surface. In the optical shadowing figures, darker colors indicated valleys. In the false-color image, green represents a neutral plane, with blues being valleys/depressions, and yellow, orange, and red as peaks. These figures illustrate pits along the linear features, surrounded by corresponding parallel raised areas.

Figure 10 and Figure 11 highlight Area 'A', which exhibited repeating, evenly spaced linear features that were oriented perpendicular to the axle longitudinal direction. These features were spaced 0.024 inches apart, consistent with the machine marks of the mating wheel bore (described in *Factual Report 22-032*). These marks were consistent with brinelling from the wheel bore surface.

Figures 12 and 13 depict differential optical shadowing and false color overlaying of the image geometry, illustrating and amplifying the morphology of the surface. The images demonstrate depressions present along the brinelling line locations. However, they were generally absent corresponding adjacent parallel peaks, which would manifest as red lines next to blue rather than the depicted green next to blue.

The outside surface of the axle wheel seat section was examined using a field emission scanning electron microscope (SEM). The brinelling features in Area 'A' are

illustrated in Figures 14 and 15, in secondary and backscattered mode, respectively.[1] These figures show that the areas with the valleys (brinelling) also exhibited areas of with lower atomic number material.

Figure 16 shows a closer view of these lower atomic mass materials, illustrated as dark black and darker gray areas. The dark gray areas exhibited concentric crescent shapes, with alternating areas of light gray. Examination of these areas using energy dispersive x-ray spectroscopy (EDS) found the dark gray material to be consistent with iron oxides. The black areas were also consistent with iron oxides which also contained higher levels of silicon, sulfur, and carbon. The light gray areas were consistent with the axle steel material.

Similar features were observed in Area 'C,' which exhibited less damage and was absent much of the brinelling features apparent in areas 'A' and 'B.' The area highlighted in Figure 17 shows the concentric crescent-shaped areas with dark gray material, found by EDS examination to be consistent with iron oxide. A closer view of an area with darker material is shown in Figure 18. This figure shows that the darker (containing less Fe) oxide was layered on top of the underlying iron oxide (dark gray).

Figure 19 shows another region in Area 'C' that exhibited similar prominent concentric crescent marks features. Figures 20 and 21 show closer views of one of the darker contrasting crescent features. The material within these features had been pressed into the axle surface, with metallic material folded over them. EDS examination of the embedded material in Figure 21 was consistent with iron oxide and ferrous alloy particles. These features were consistent with oxidized wear debris typical of fretting wear between two faying surfaces.

Parallel to the axle section in Figure 5, cross sections of the axle surface were mounted in vacuum-impregnated cold epoxy, ground, and polished. Various surface locations were examined in the as polished and etched state (using a 2% Nital solution).[2]

Figures 22 and 23 show a cross-section through the inboard part of Area 'A.' While these figures do not show pits or inward-propagating cracks, a layer of nonuniform material was present on the surface, consistent with the axle material, indicating localized plastic deformation of the surface.

Figure 24 shows a closer view of one of the brinelling marks. This figure shows a generally flat depression in the surface, with no corresponding peaks on the feature

---

[1] Backscattered electrons: SEM micrographs produced using backscattered electrons display contrast that is associated with the atomic numbers of the elements in the micrograph. Materials containing elements with higher atomic numbers visually appear lighter relative to other materials containing elements with lower atomic numbers.

[2] 2% Nital – a mixture of 2% concentrated nitric acid (HNO_3) in ethanol (C_2H_5OH).

edges. However, the edges did exhibit localized folds, oriented parallel to the surface. This fold consisted of areas with small cracks, approximately 5 – 10 μm (2 – 4 x 10^{-4} inches) in length. A brinelling mark in Area 'C' exhibited a similar shape, with a flat depression and two opposite-oriented longitudinal cracks underneath folds on the edges. This brinelling feature also contained dark gray material, consistent with iron oxide.

The surface also exhibited entrained particles, which contrasted darker in optical micrographs. Figures 27 and 28 show some of these particles observed on Area 'A' surface. The particle to the right was associated with an underlying discontinuity consistent with a deformation fold. This feature exhibited tiny secondary cracks emanating from the particle. Similar particles were observed on the surface in Area 'B.' EDS examination of these particles found them to be consistent with iron oxide, with higher levels of silicon, carbon, and chromium.

Area 'C' also exhibited surface oxide particles, as illustrated in Figures 31 through 34. This area was not consistent with individual large particles but rather a series of smaller debris fragments clustered along the surface. Figure 34 shows a closer view of one of the large debris areas, exhibiting interior fracturing and adjacent microstructure deformation consistent with compression into the axle surface. Determined to be consistent with iron oxide, this debris was consistent with that which typically had accumulated in bands of fretting wear.

The area described as the 'band of fretting' in Figure 5 exhibited more surface distortion than in inboard Areas A through C. Figure 35 shows a typical area displaying an undulating surface profile with underlying microcracking. These cracks were oriented parallel to the surface of the axle wheel seat. The largest crack exhibited a depth of 0.0005 inches and a length of 0.0015 inches (0.013 mm depth and 0.038 mm long).

Small pits were also observed in the band of fretting wear. Figure 36 shows an area with a small pit. A microcrack had begun to propagate towards the right in the Figure. A closer examination of a similar site in an SEM is illustrated in Figure 37. This Y-shaped pit was adjacent to a circular pit, with an area of folded surface material between them. Cracks were observed emanating from both pits, oriented parallel to the axle surface. Figure 38 shows a closer view of the Y-shaped pit, with oxide in the valley. This material was found to be consistent with iron oxide, containing minor amounts of chlorine and phosphorus.

Besides pits, folds, and cracks observed on the surface, the adjacent microstructure of the axle had been altered adjacent to the surface. Figures 39 and 40 provide closer views of the surface in the etched condition. While the interior (bottom of the figures) exhibited a more equiaxed appearance, consistent with prior austenite grain boundaries, the material near the surface revealed a curved and flattened

morphology. These microstructural features were bent towards the outboard direction of the axle. There were no indications of a white surface layer, which could indicate localized overheating.

The cross-section of the band of fretting wear was examined using an automatic microhardness indenter per ASTM E384.[3] Figure 41 shows the hardness data plotted against distance from the surface. From previous testing of the axle, the average hardness of the material was 27 HRC (equivalent to 290 HK_{500} per ASTM E140).[4] The data indicate that the surface exhibited a lower hardness, followed by a slightly higher hardness subsurface, before averaging towards 290 HK_{500} at a depth of 0.012 inches. These data indicate that the surface deformation and fretting wear altered the local mechanical properties of the axle.

Submitted by:

Erik M. Mueller
Materials Research Engineer

[3] ASTM E384 – *Standard Test Method for Knoop and Vickers Hardness of Materials*. ASTM International, West Conshohocken, PA
[4] ASTM E140 – *Standard Hardness Conversion Tables for Metals Relationship Among Brinell Hardness, Vickers Hardness, Rockwell Hardness, Superficial Hardness, Knoop Hardness, and Scleroscope Hardness*. ASTM International, West Conshohocken, PA

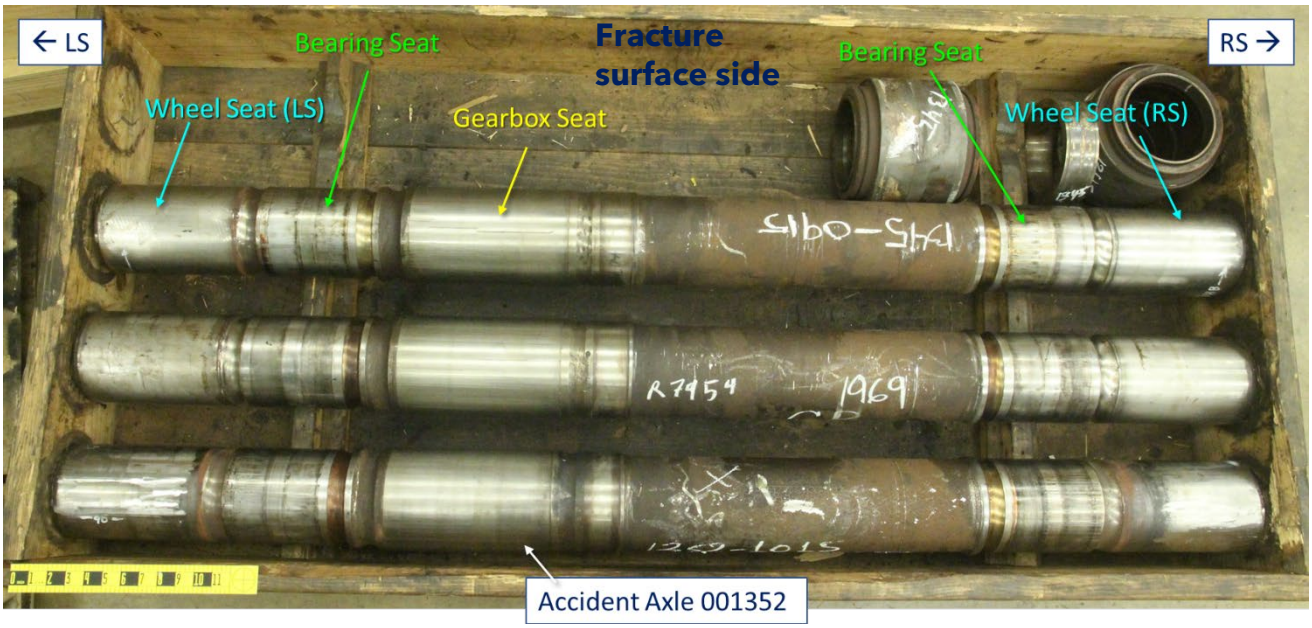

Figure 1. View of the three axles as received. The axle on the bottom was examined in this report.

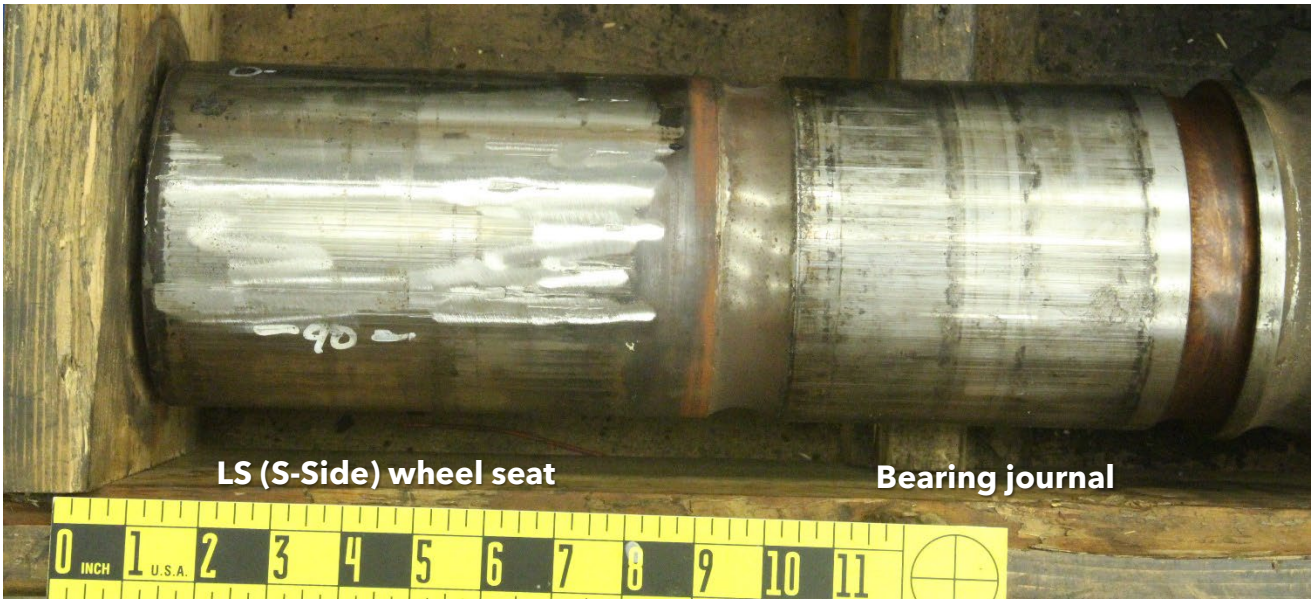

Figure 2. The left side wheel seat and bearing journal from the accident axle, 1352, as received.

Figure 3. The right side wheel seat on the accident axle, as received.

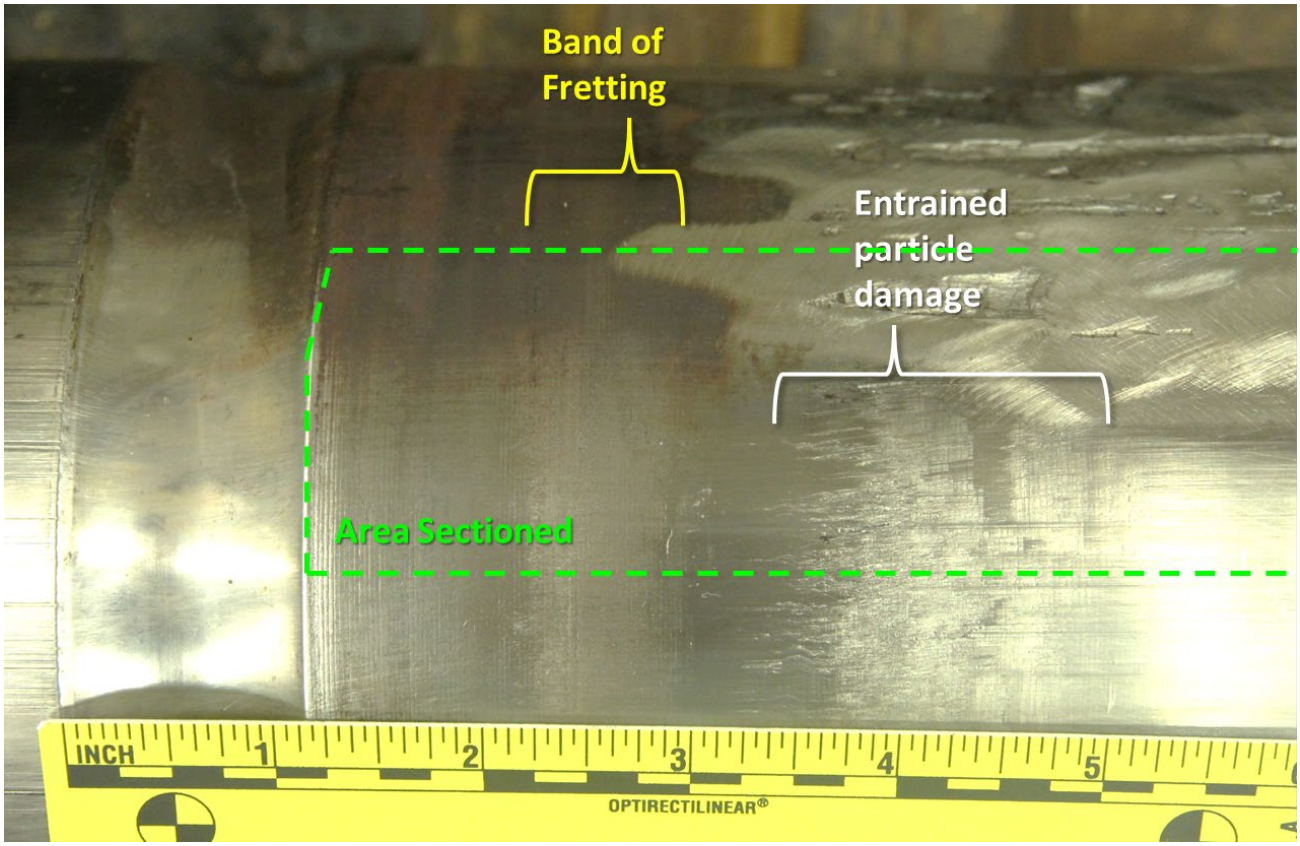

Figure 4. Annotated views of the area of fretting wear, areas of entrained particle damage, and the boundaries of the sectioned axle area.

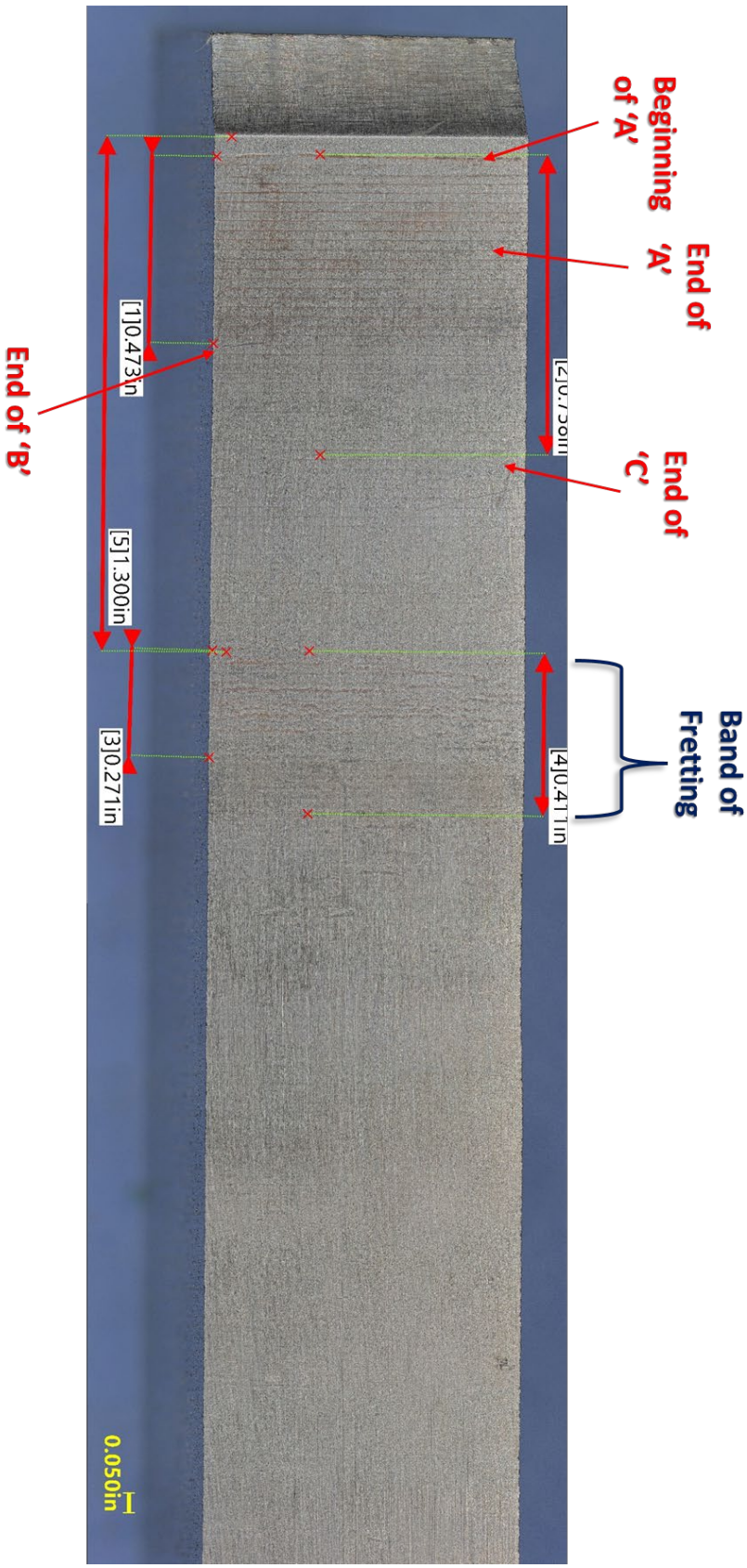

Figure 5. Montage of the surface of the right-side axle section, annotated to show the various regions and their distances from the inboard groove (top of figure).

Figure 6. View of the most severe band of fretting wear on the axle wheel seat surface.

Figure 7. Closer view of the fretting wear features in **Figure 6**.

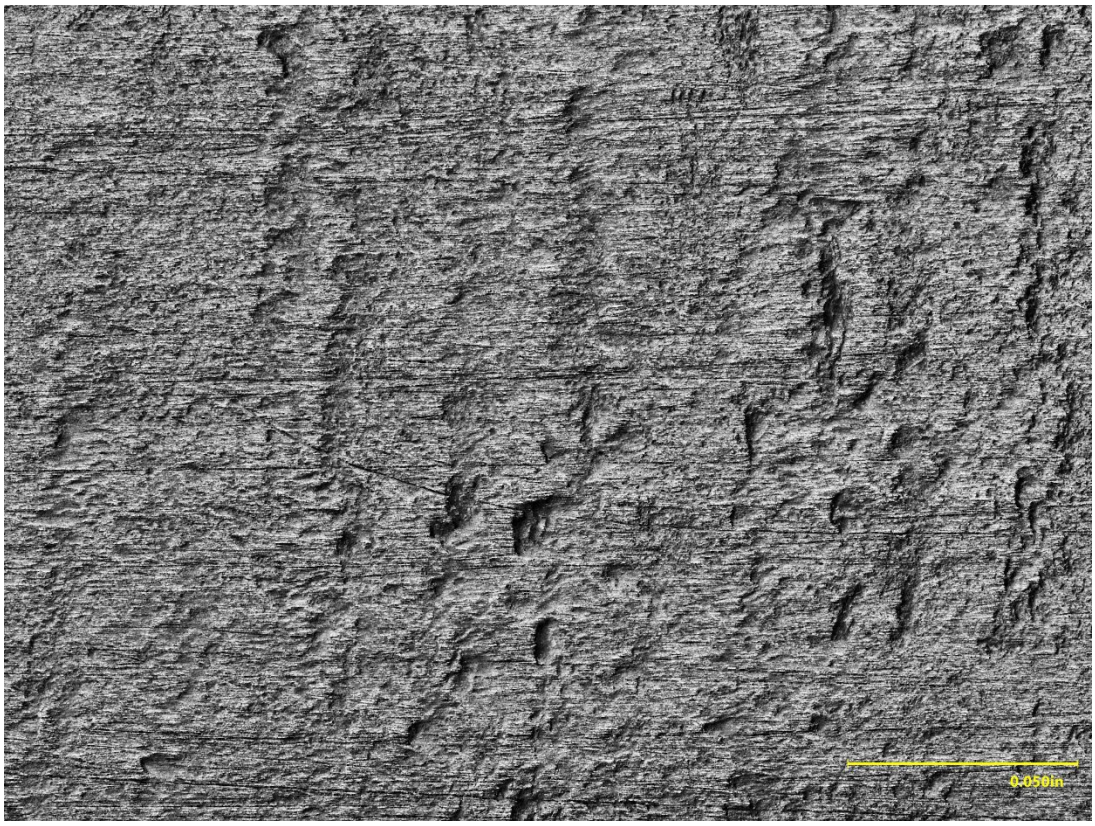

Figure 8. Differential optical shadowing image of the area in **Figure 7**.

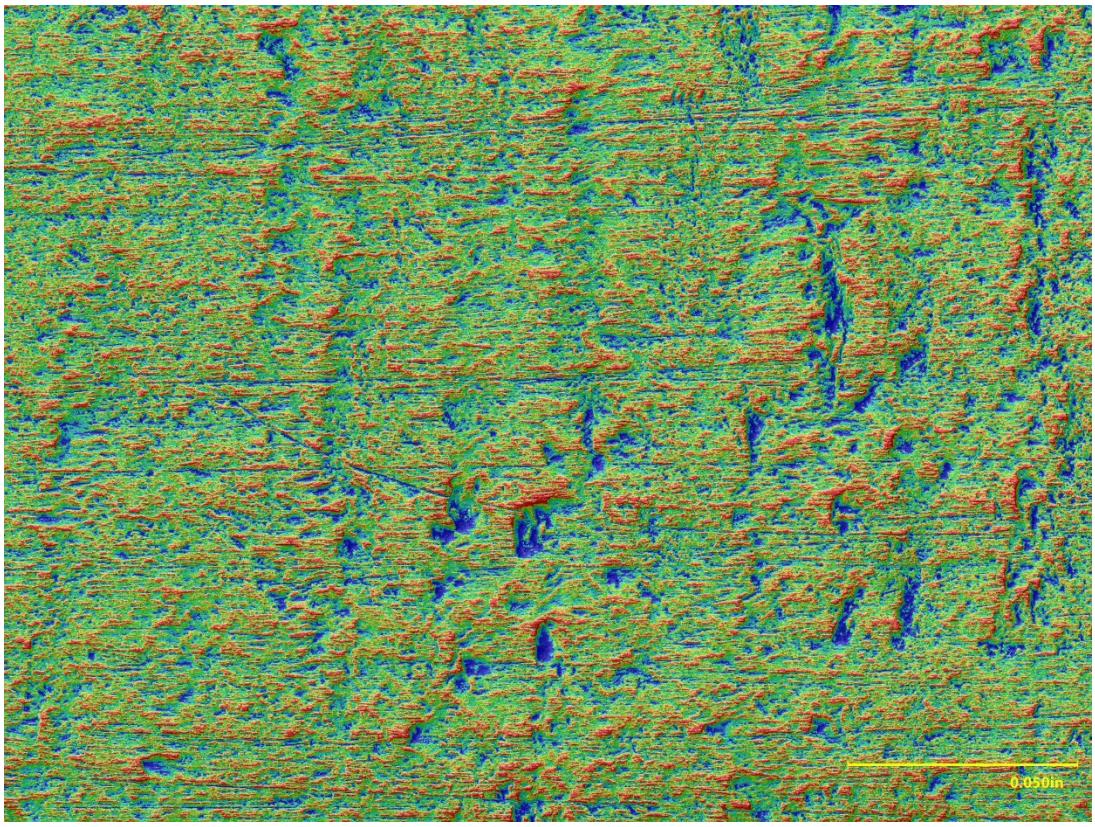

Figure 9. False color image of peaks (red) and valleys (blue) in the surface topography of **Figure 8**.

Figure 10. View on the inboard corner of Area A, showing brinelling of the surface from the wheel bore.

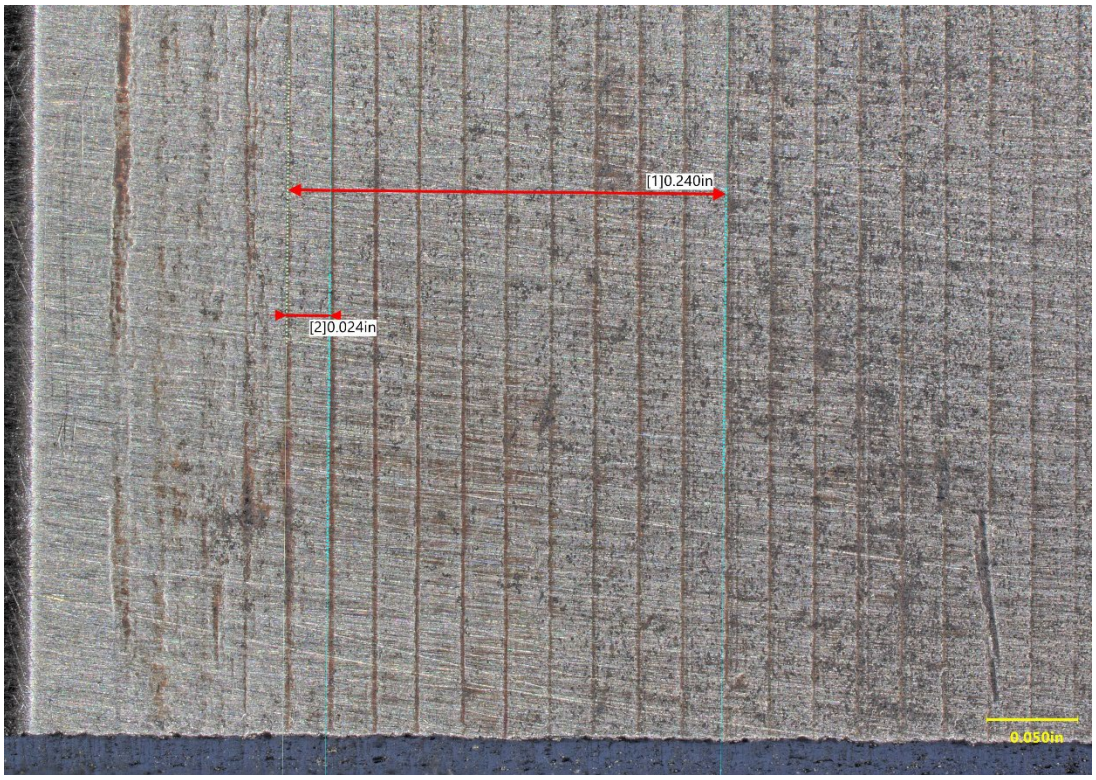

Figure 11. Figure 10 annotated to show several measurements between marks.

Figure 12. Closer view of the brinelling marks in **Figure 11**.

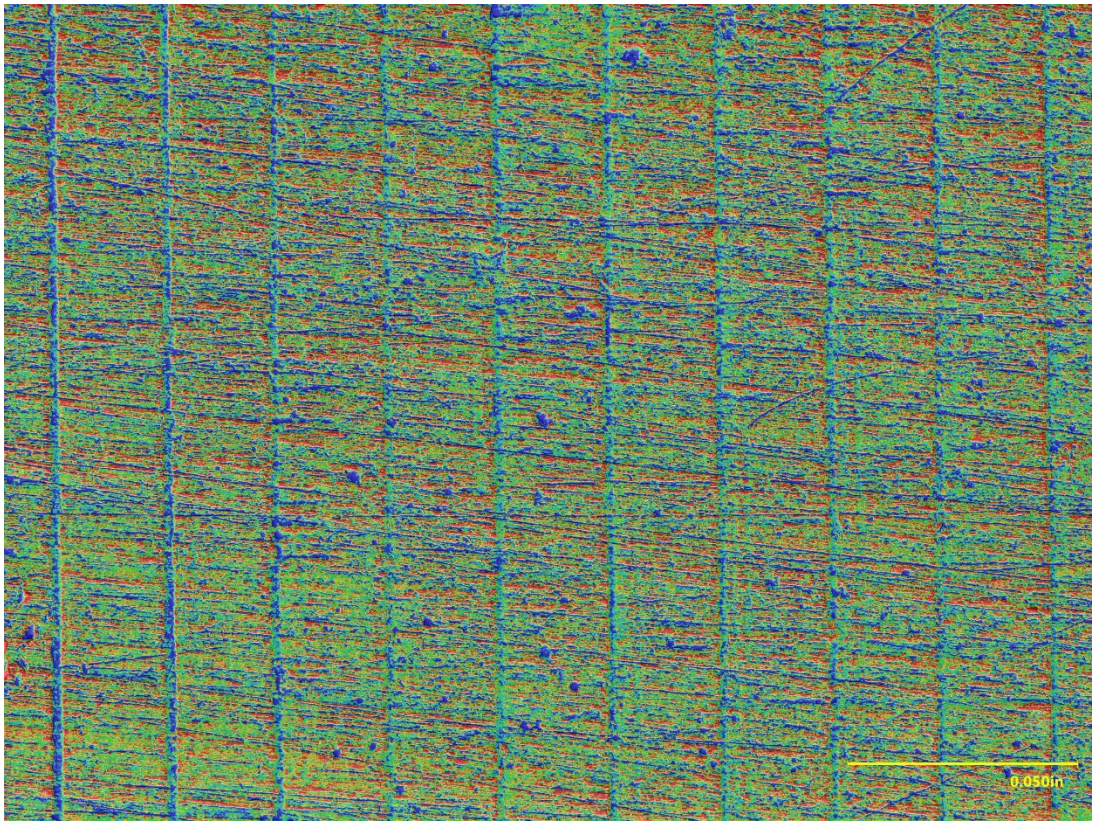

Figure 13. False color image of peaks (red) and valleys (blue) in the surface topography of **Figure 12**.

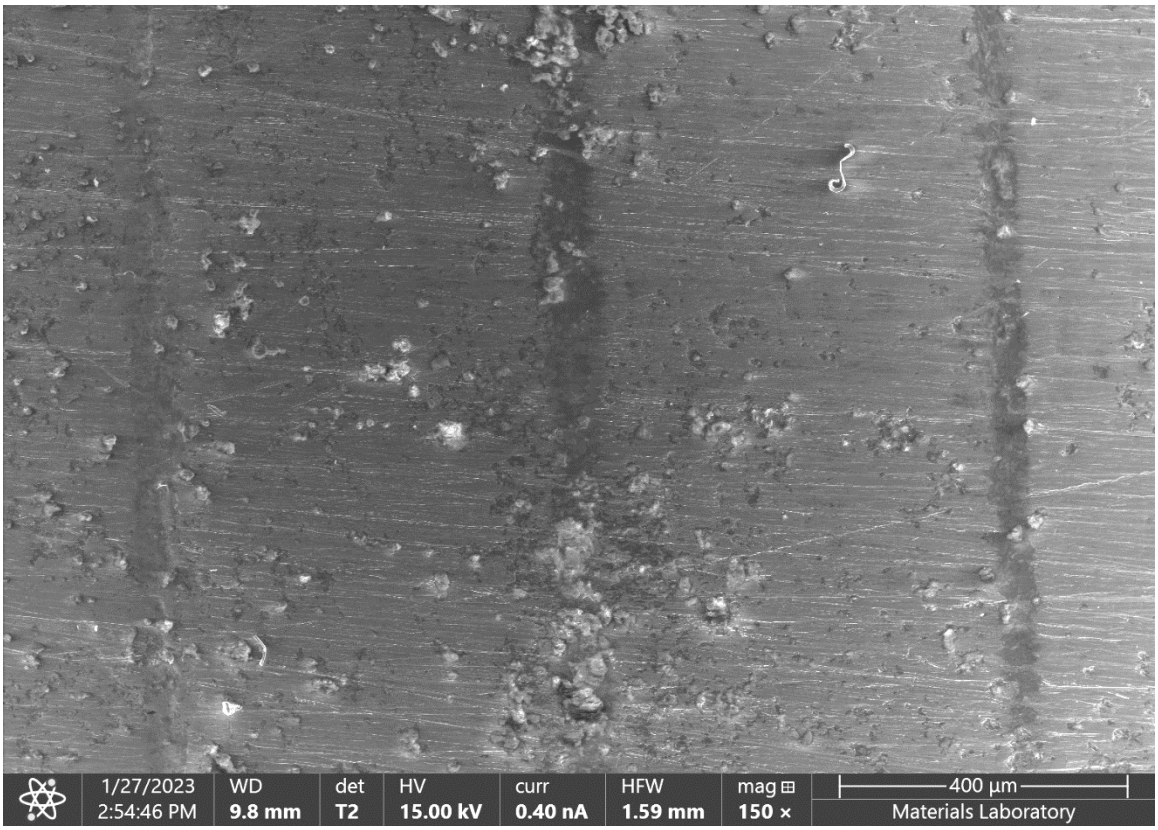

Figure 14. Secondary electron (SE) micrograph of brinelling in Area A.

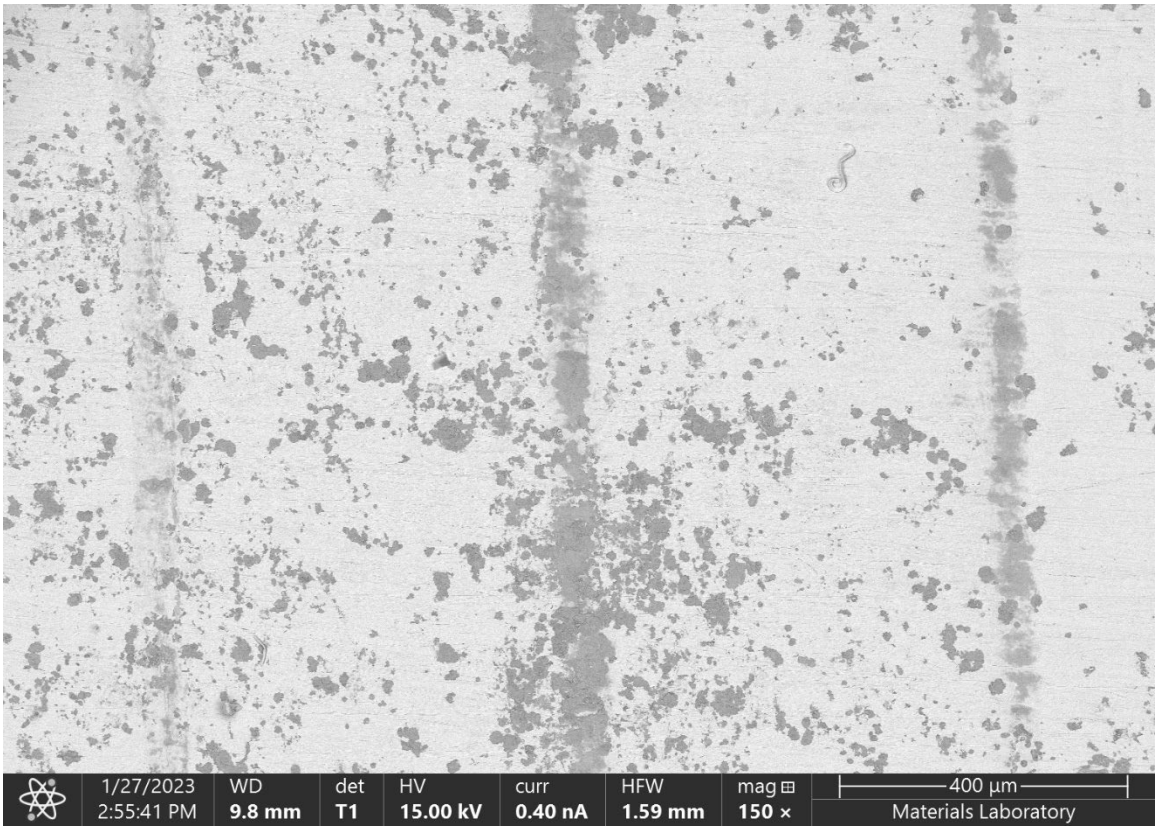

Figure 15. Backscattered electron (BE) micrograph of brinelling in Area A.

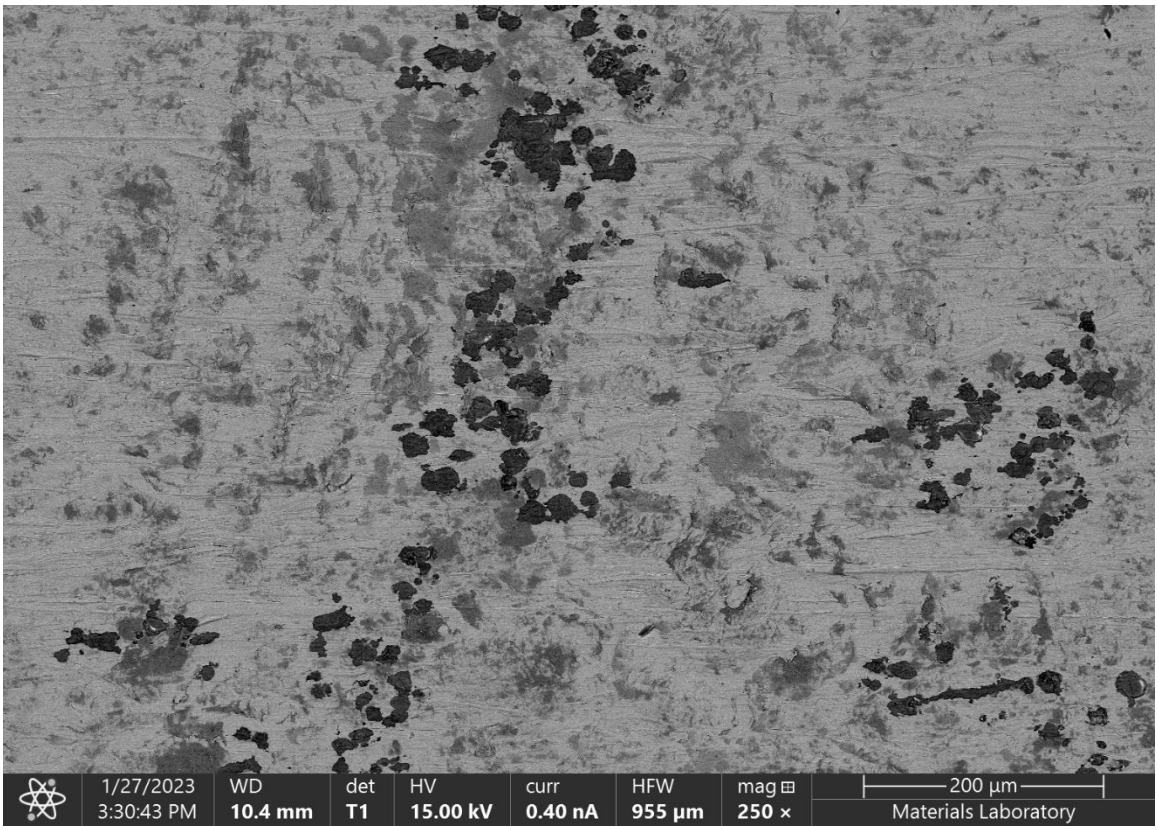

Figure 16. BE micrograph of showing a closer view of the different surface phases in Figure 15**.**

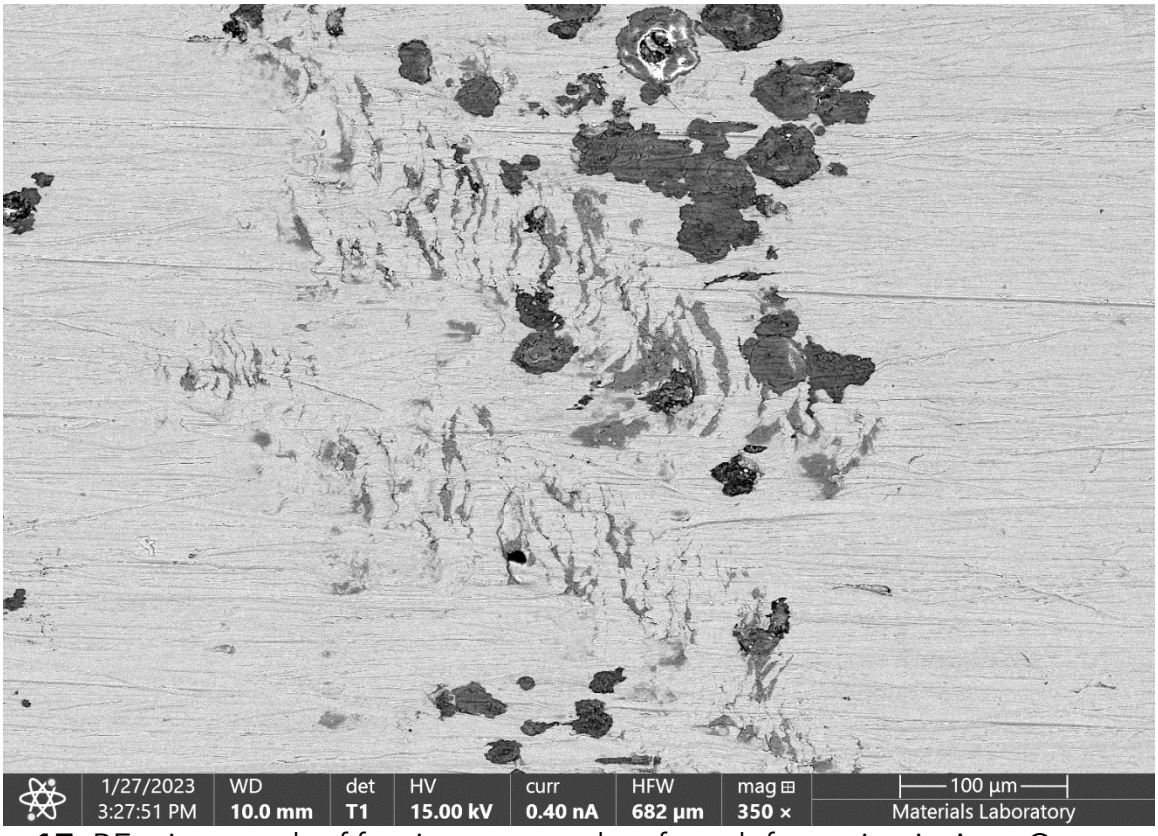

Figure 17. BE micrograph of fretting wear and surface deformation in Area C.

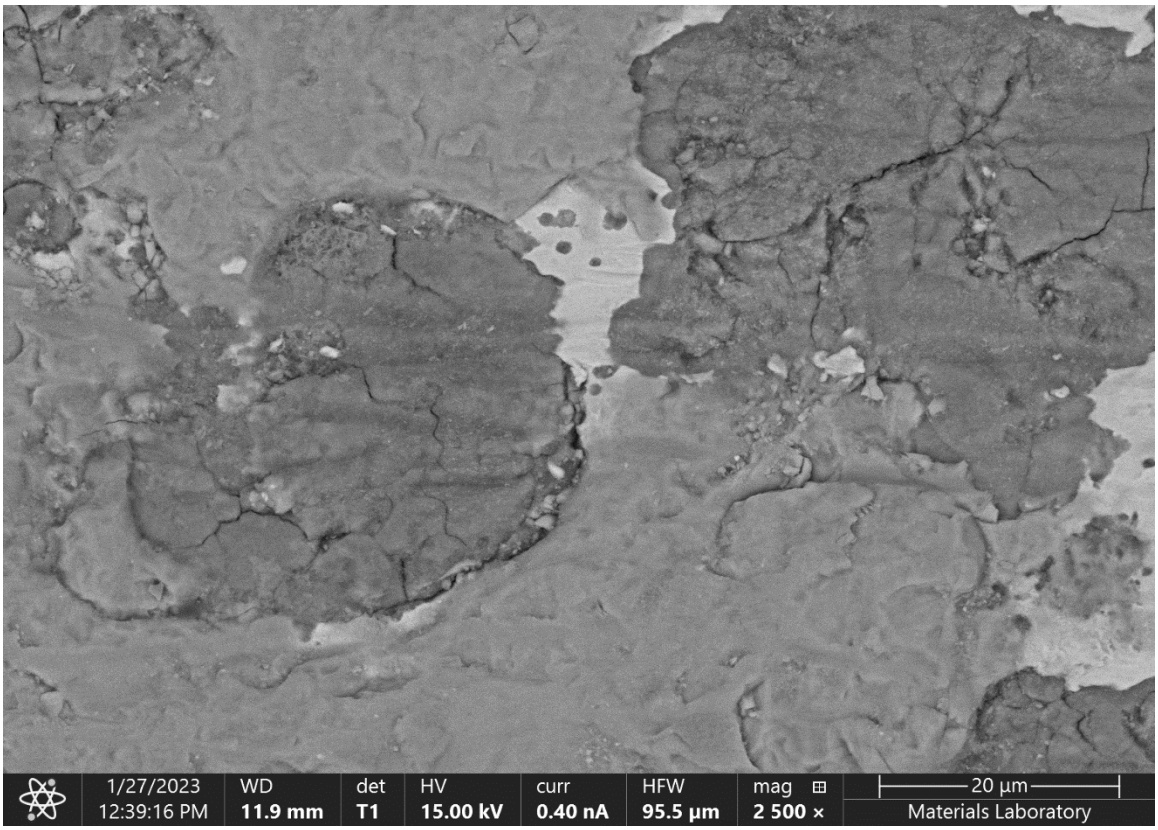

Figure 18. BE micrograph of layers of oxide from **Figure 17**.

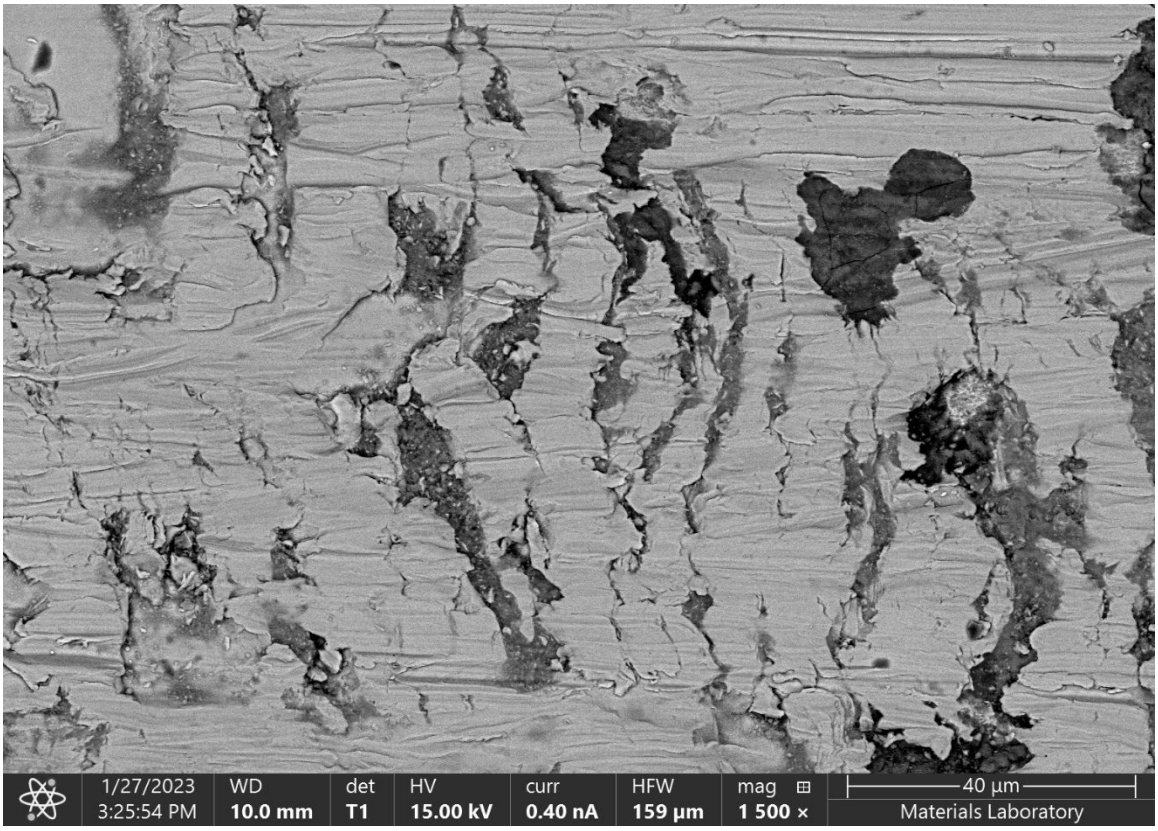

Figure 19. BE micrograph of folds, deformation, and entrained oxidation in Area C.

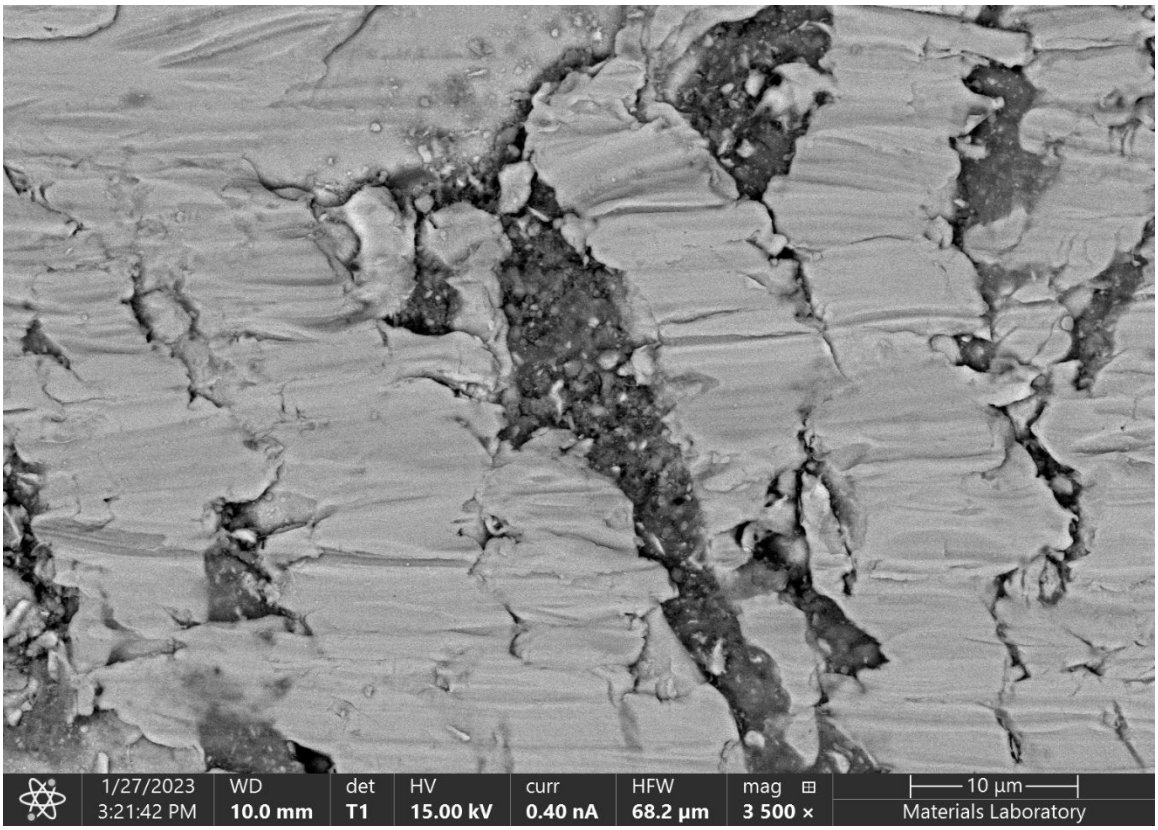

Figure 20. BE micrograph of a closer view of the features in **Figure 19**.

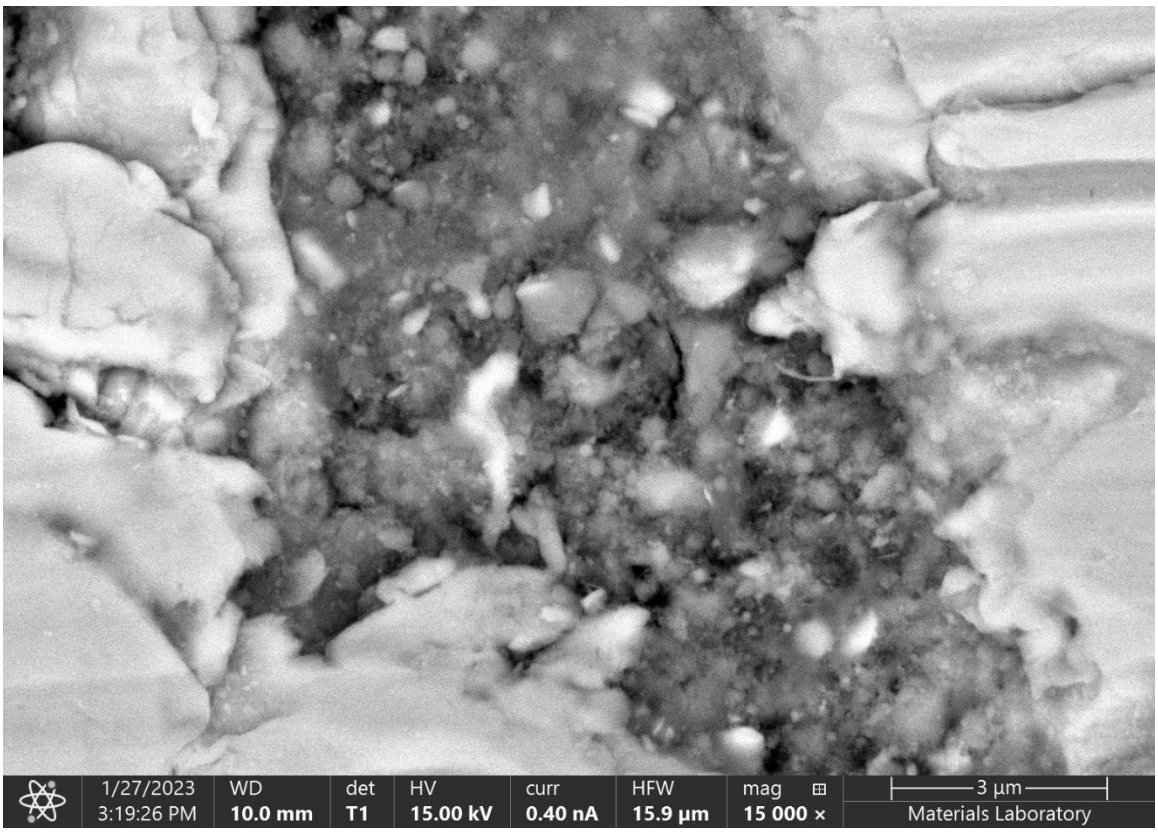

Figure 21. BE micrograph of the entrained oxide in **Figure 20**.

Figure 22. Bright-field (BF) optical micrograph of the beginning of A (~500X, as polished).

Figure 23. Bright-field (BF) optical micrograph of the beginning of A (~500X, etched 2% Nital).

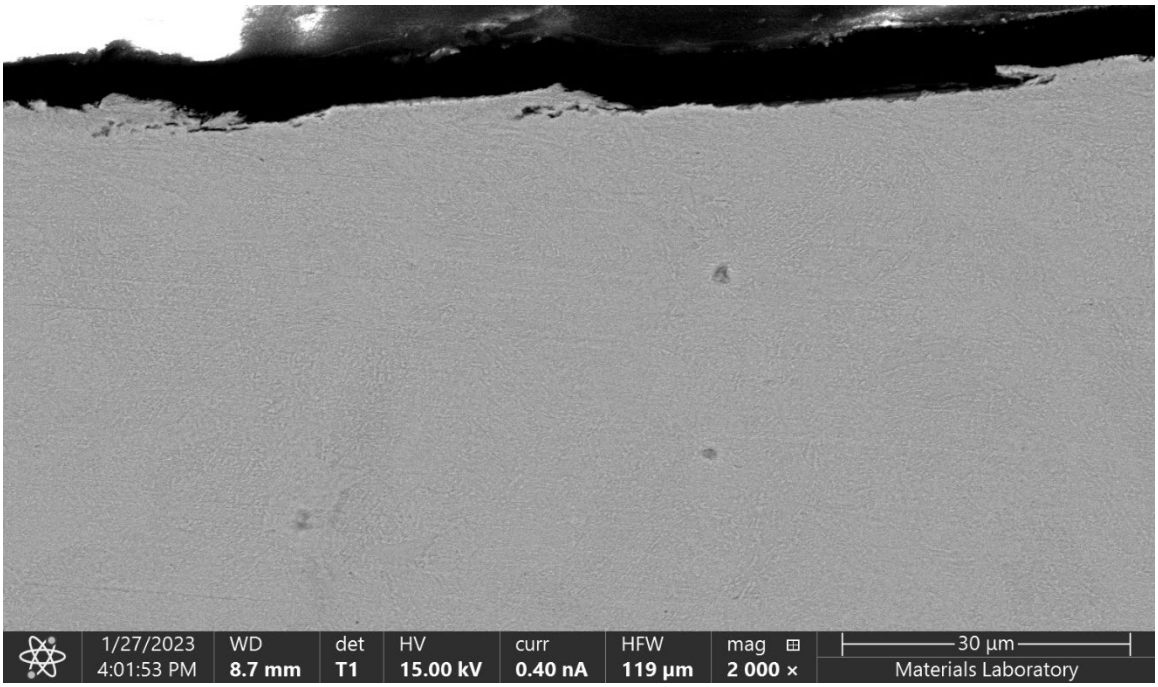

Figure 24. Backscattered electron (BE) micrograph of a cross section of brinelling marks in Area A.

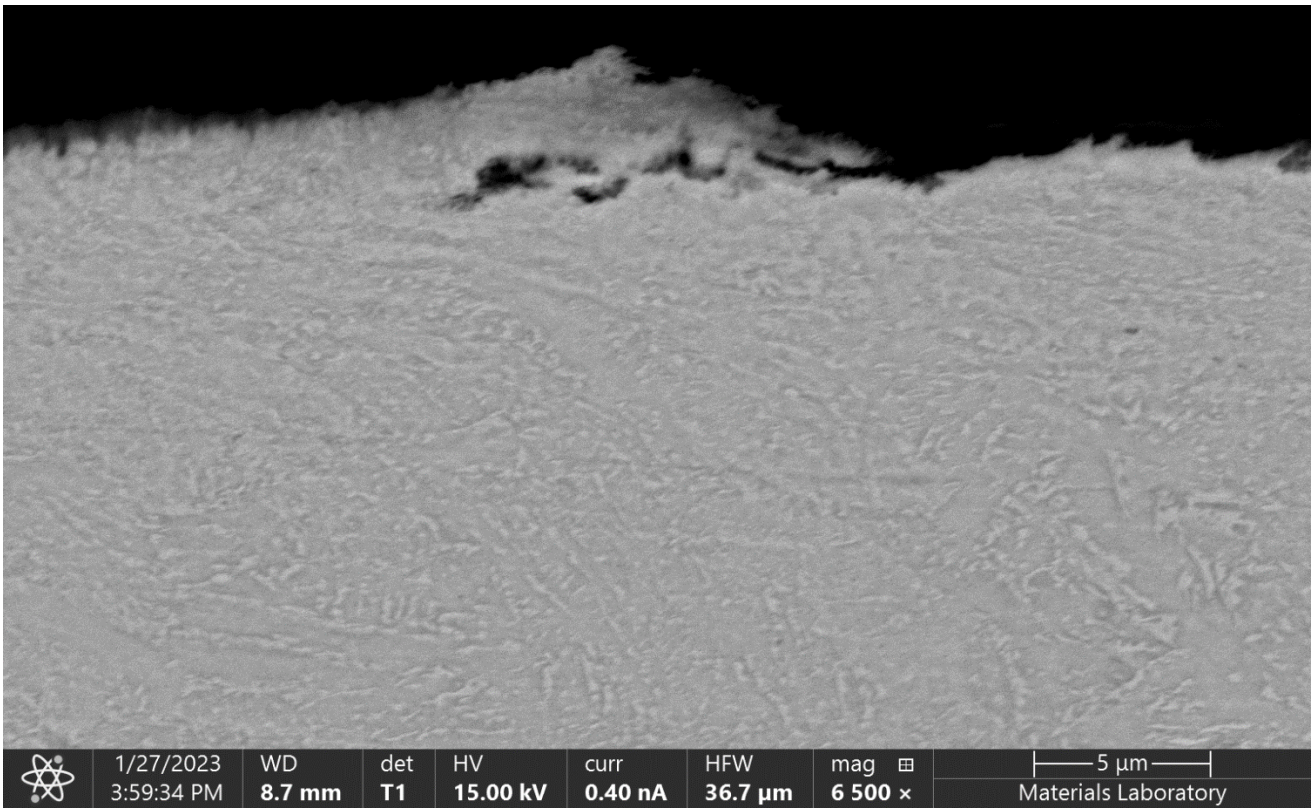

Figure 25. BE micrograph of a closer view of the left side of Figure 16.

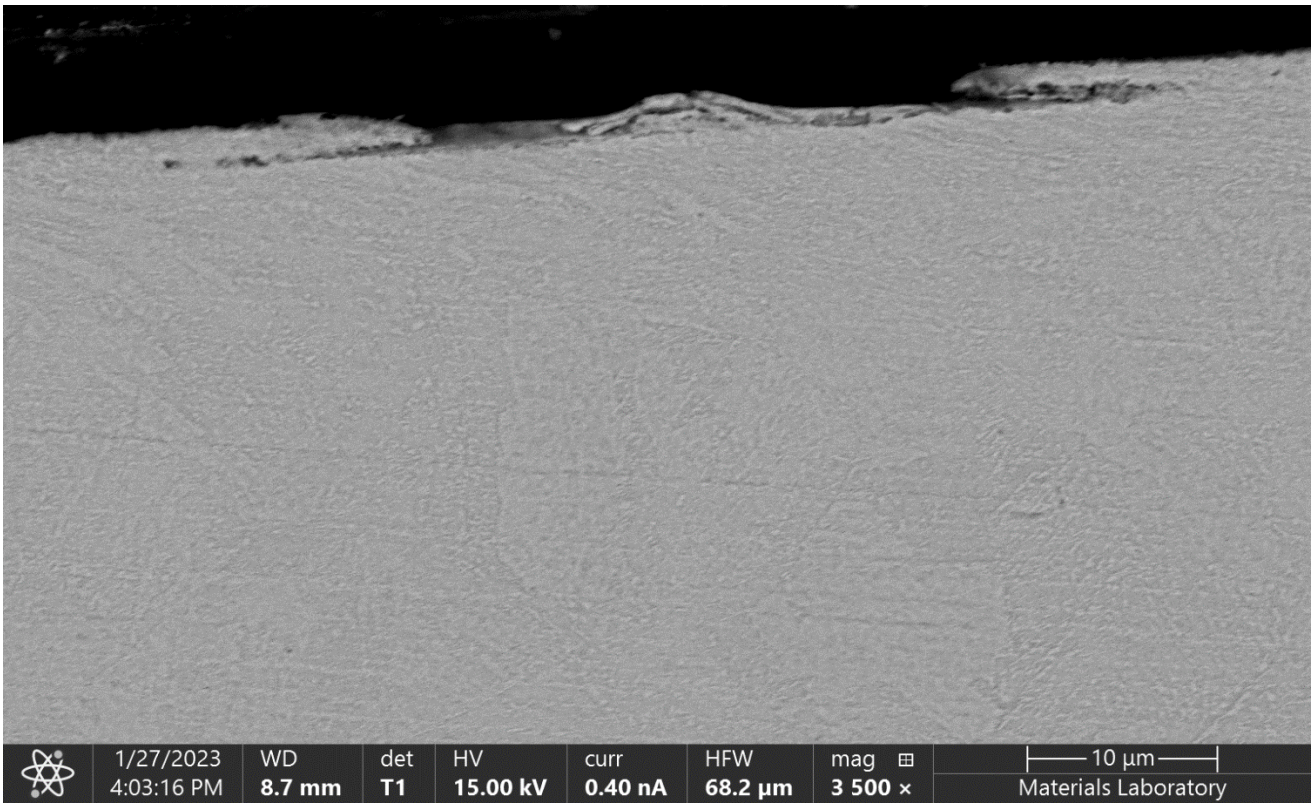

Figure 26. BE micrograph of a cross section of brinelling in Area C.

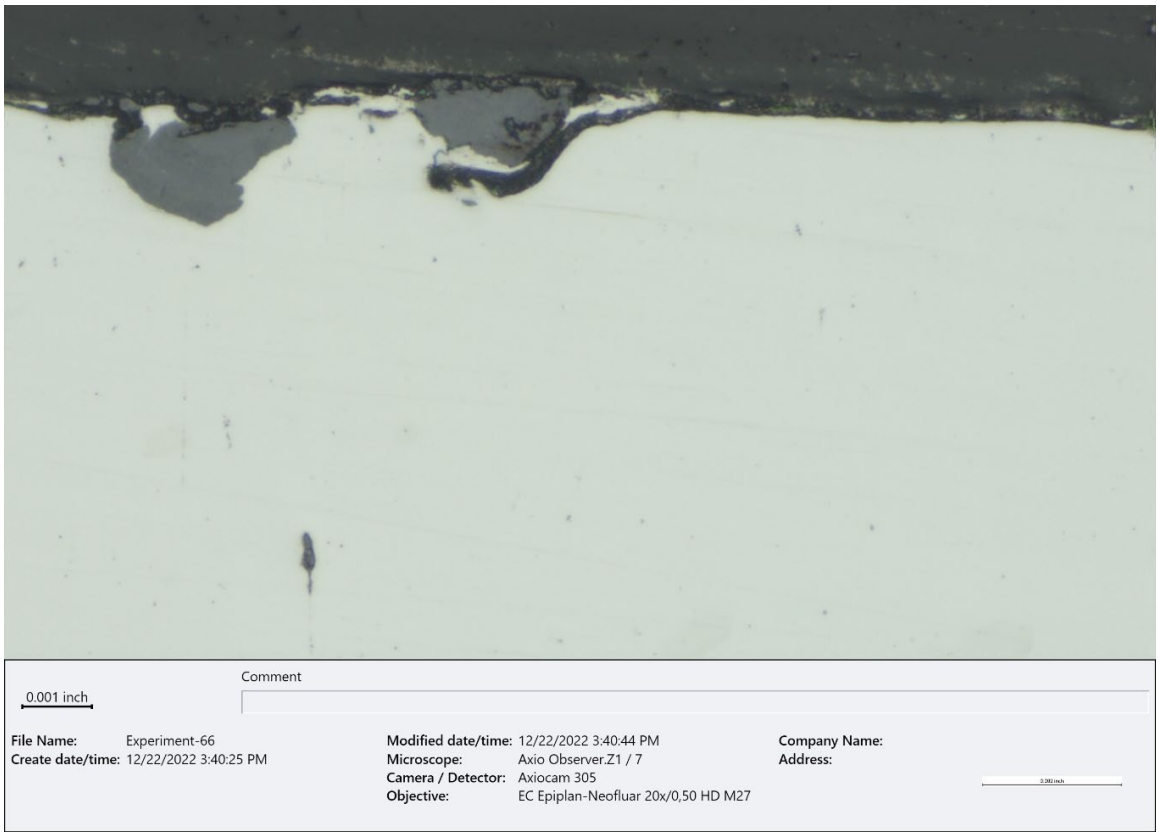

Figure 27. BF optical micrograph of the embedded particles in the end of A (~500X, as polished).

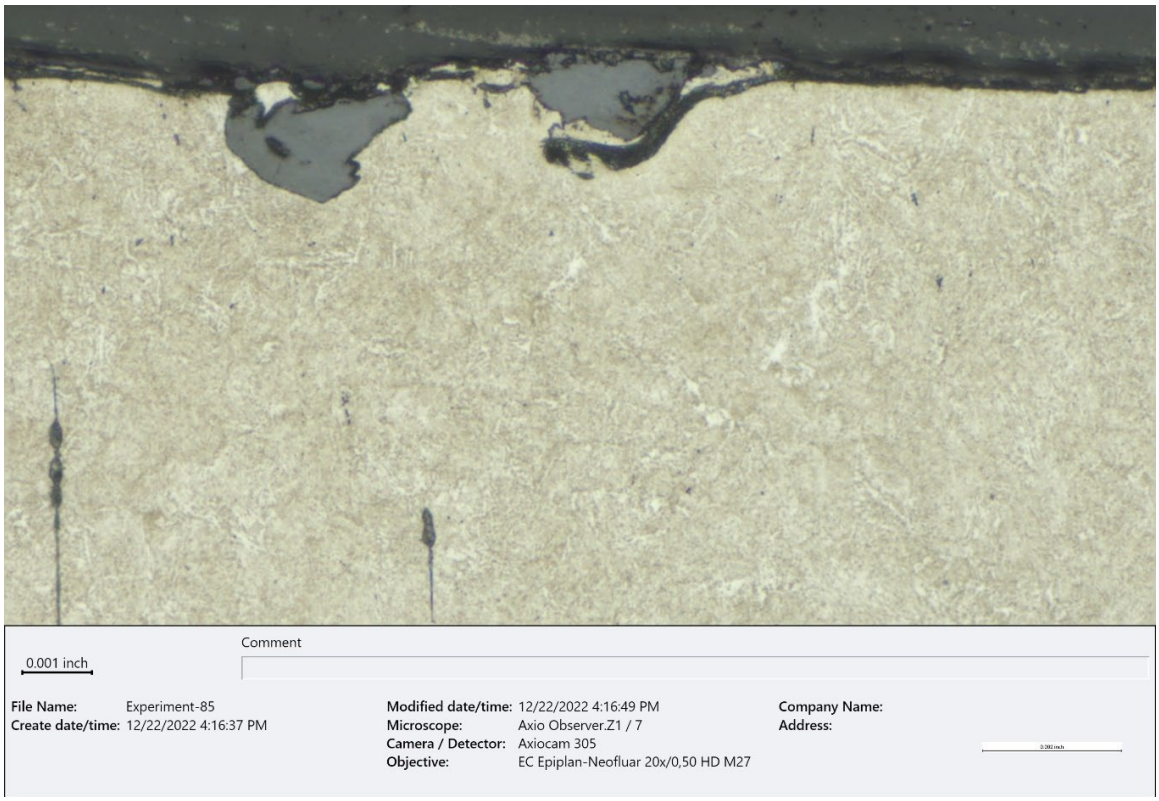

Figure 28. BF optical micrograph of embedded particles in A (~500X, etched 2% Nital).

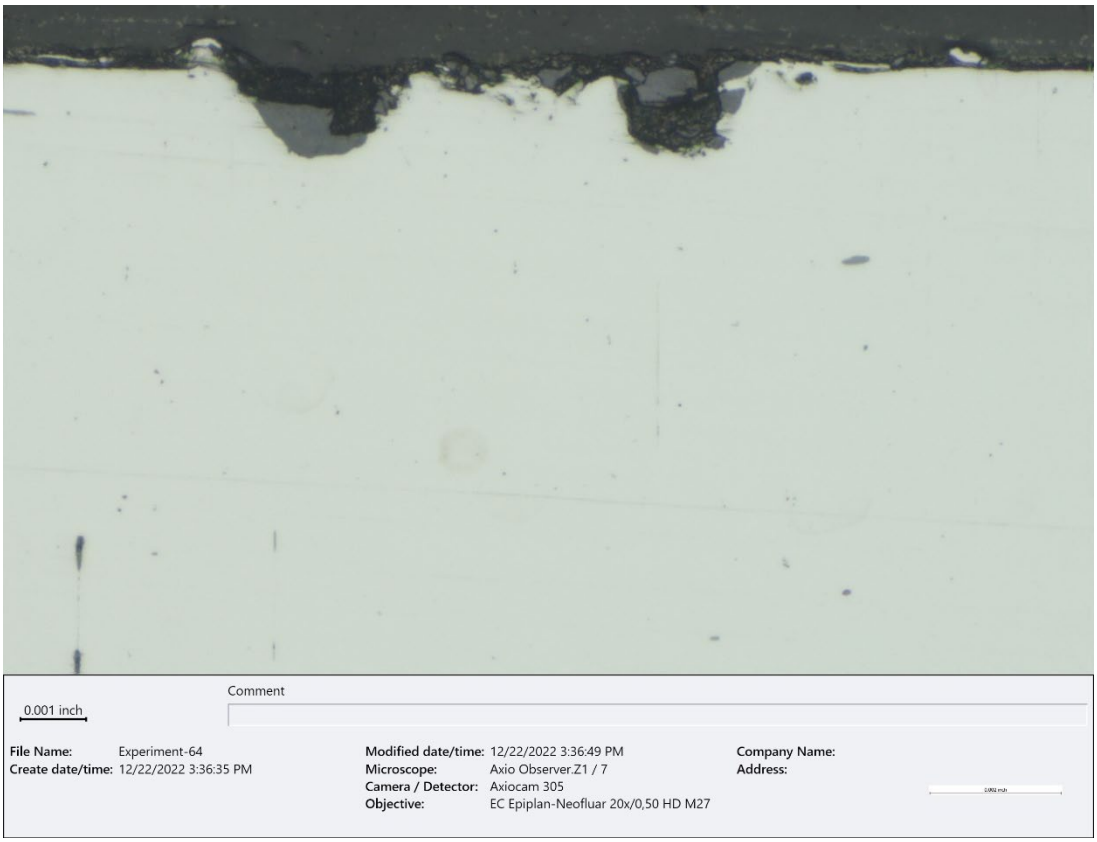

Figure 29. BF optical micrograph of embedded particles in B (~500X, as polished).

Figure 30. BF optical micrograph of embedded particles in B (~500X, etched 2% Nital).

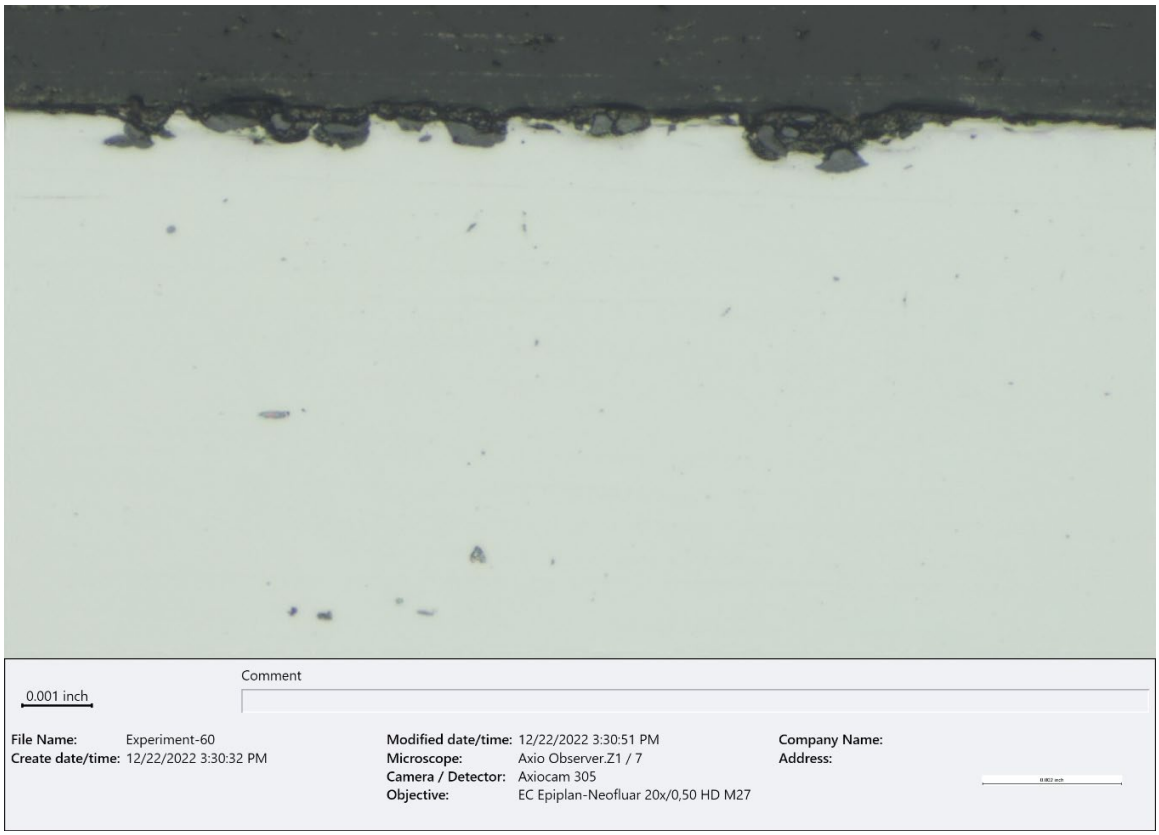

Figure 31. BF optical micrograph fretting wear damage in Area C (~500X, as polished).

Figure 32. BF optical micrograph of fretting wear in Area C (~500X, etched 2% Nital).

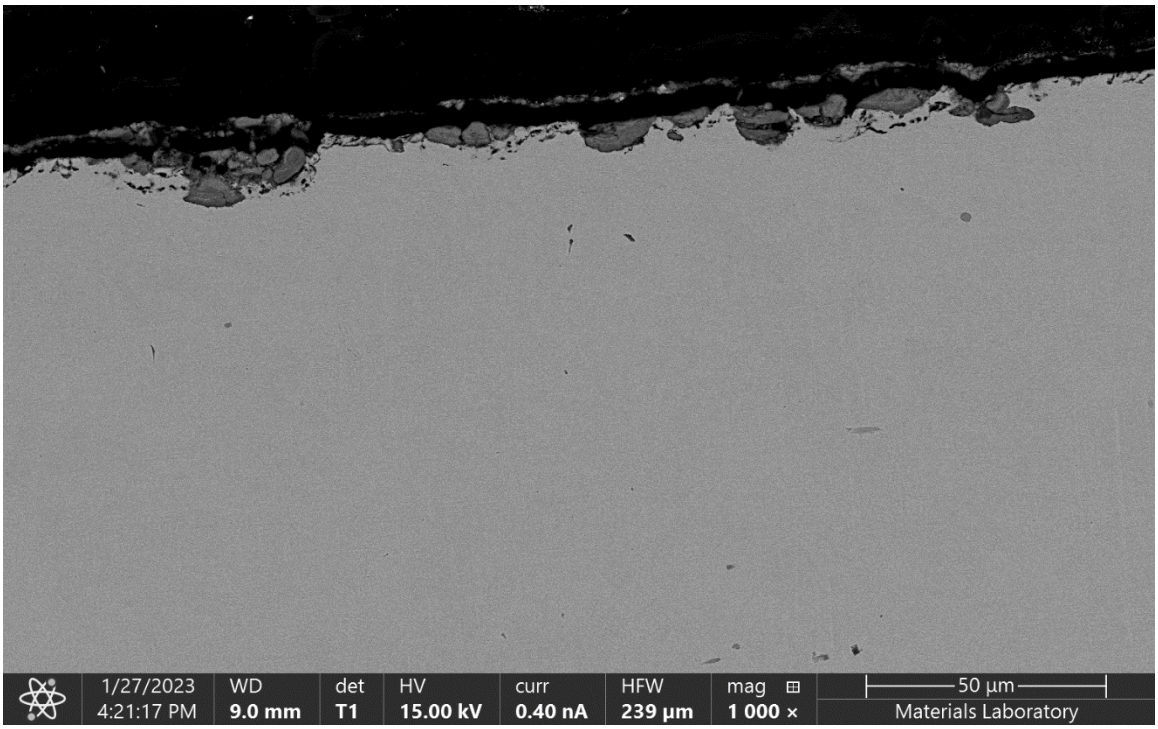

Figure 33. BE micrograph of fretting wear damage in Area C.

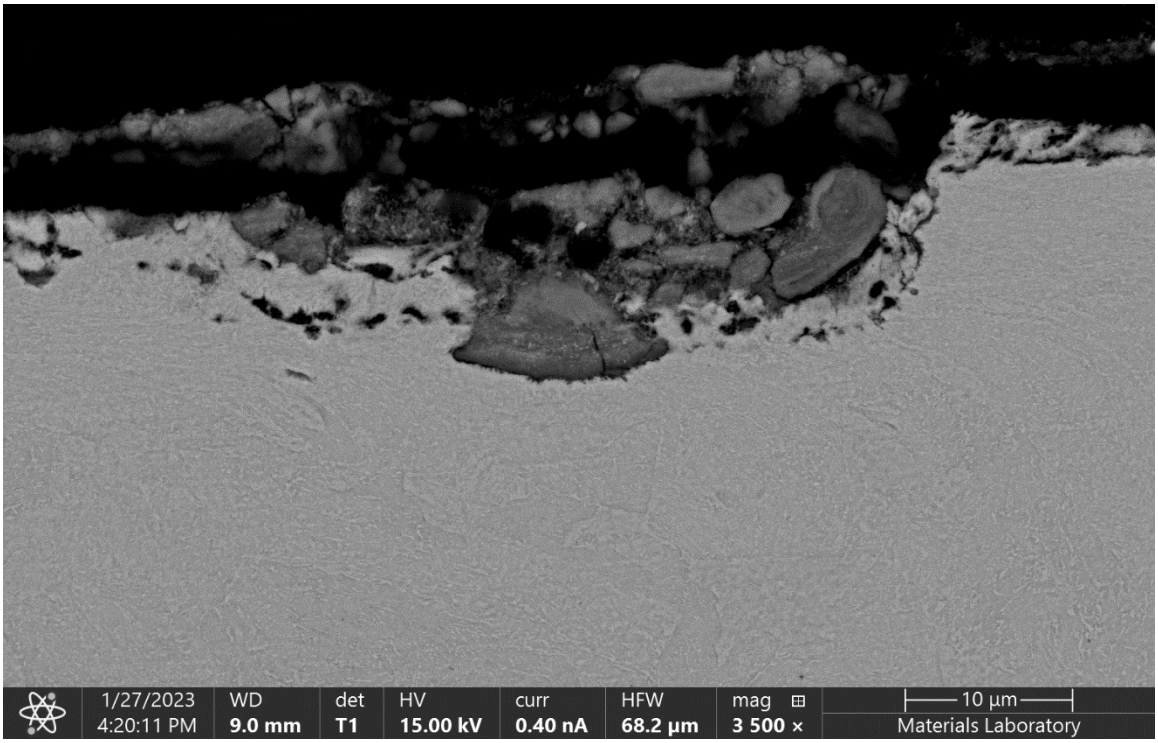

Figure 34. BE micrograph of a closer view of a surface particle in Figure 33.

Figure 35. BF optical micrograph of fretting wear in the outboard axle areas (~500X, as polished).

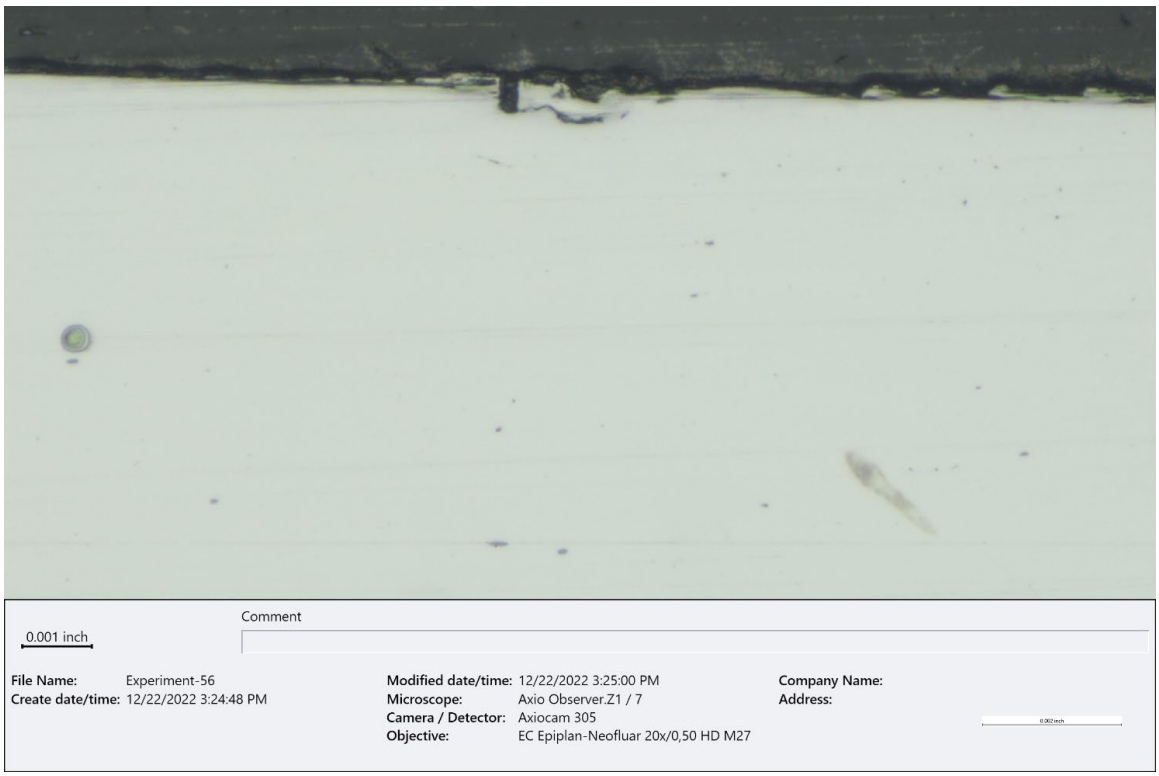

Figure 36. BF optical micrograph of a subsurface crack in a fretting wear area (~500X, as polished)

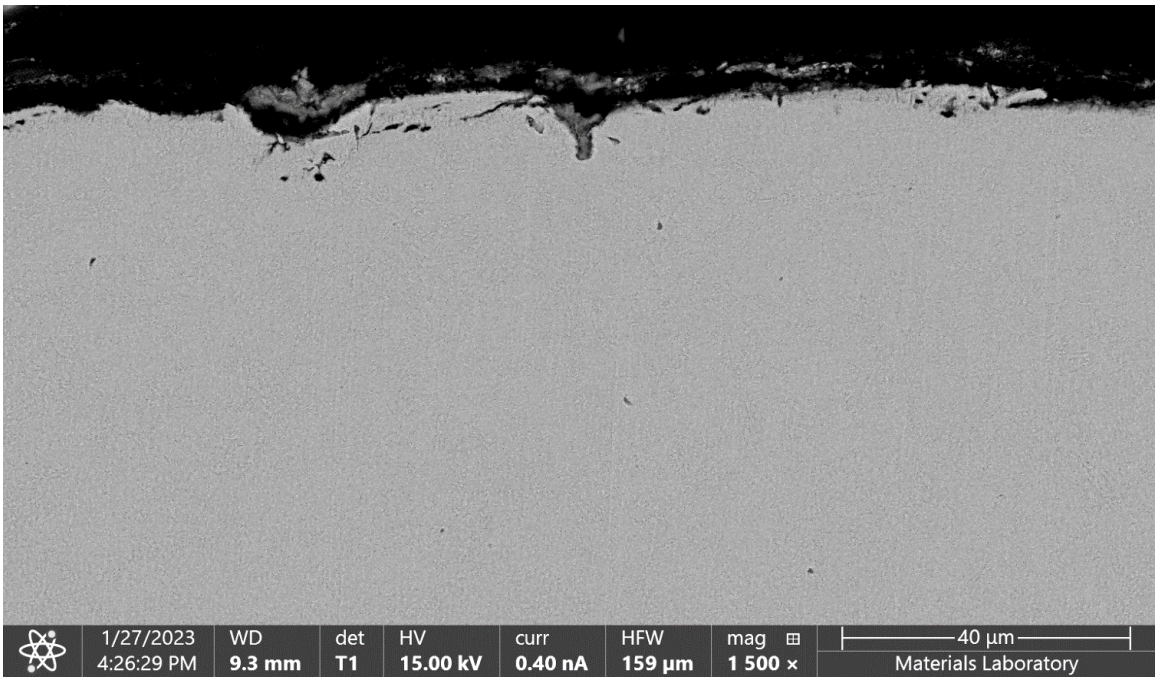

Figure 37. BE micrograph of surface damage, oxidation, and subsurface cracking under areas of surface fretting wear.

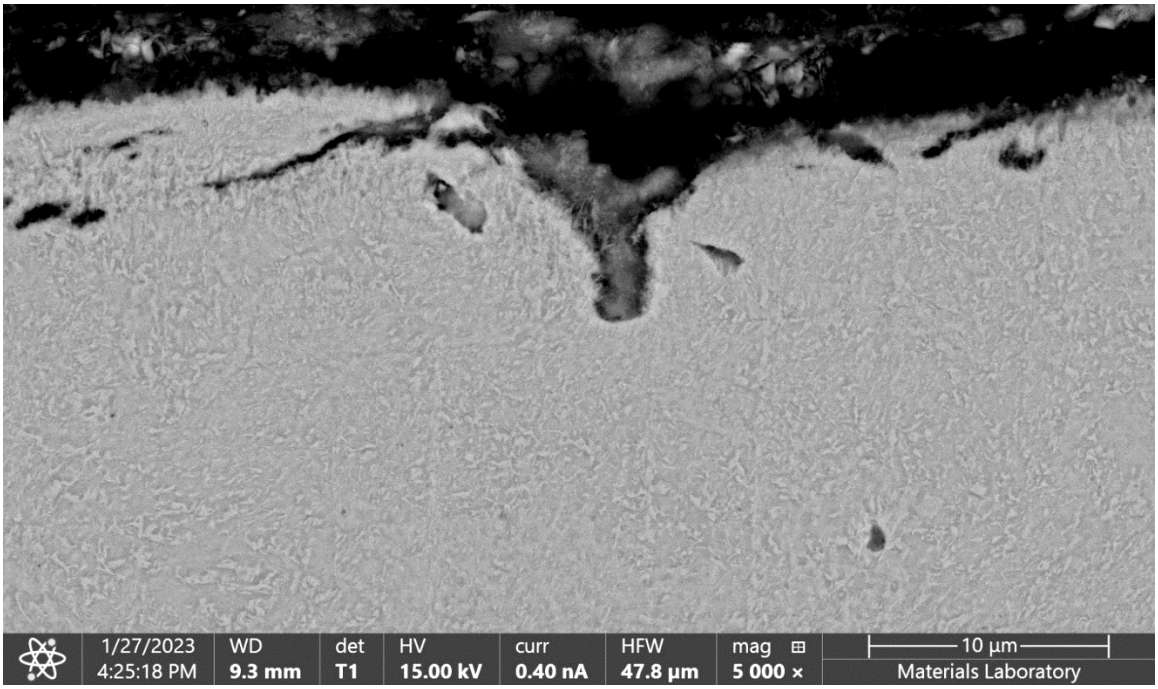

Figure 38**.** BE micrograph of the depression feature in **Figure 37**.

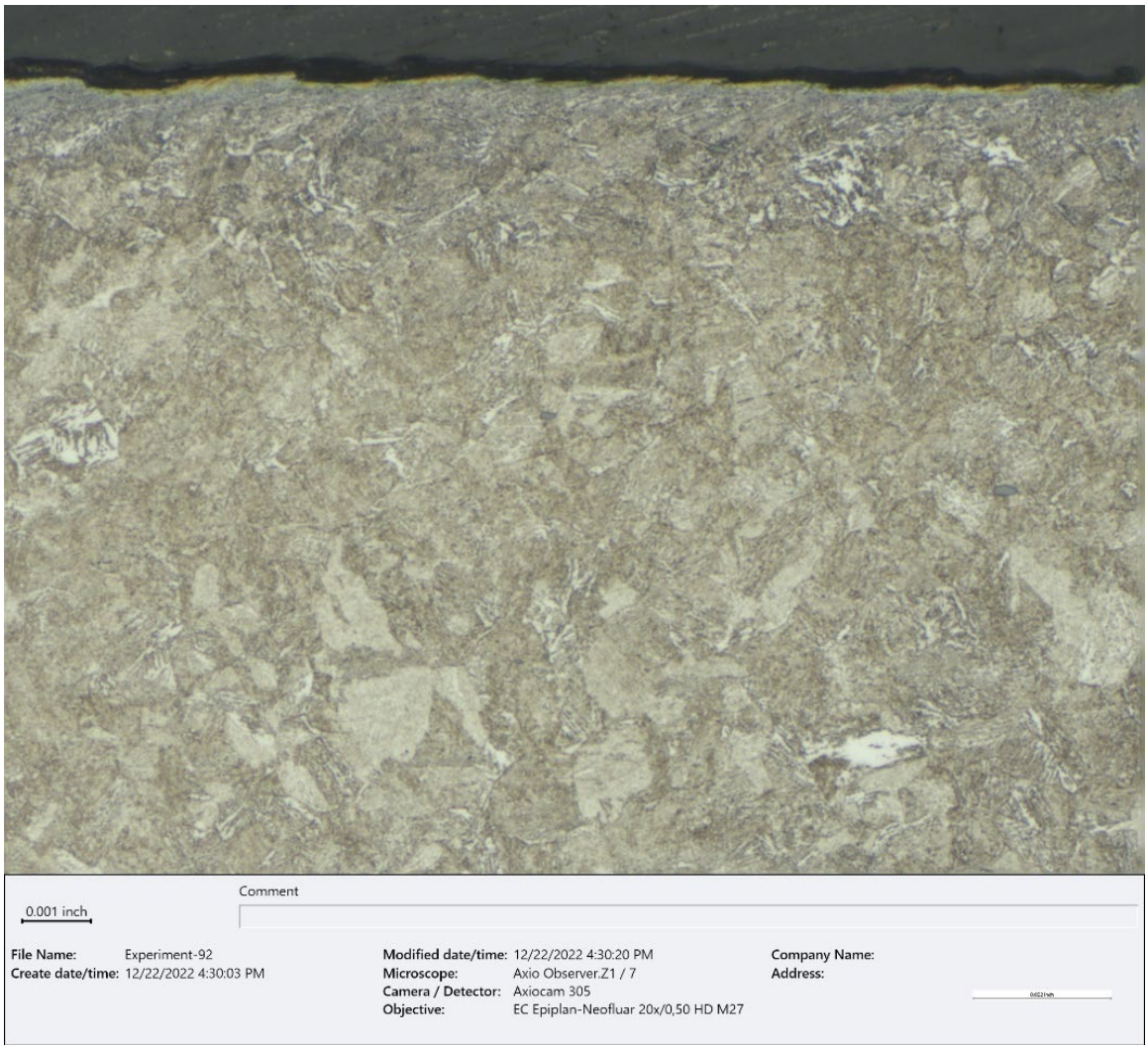

Figure 39. BF optical micrograph, etched to show grain deformation near the surface (~500X, etched 2% Nital).

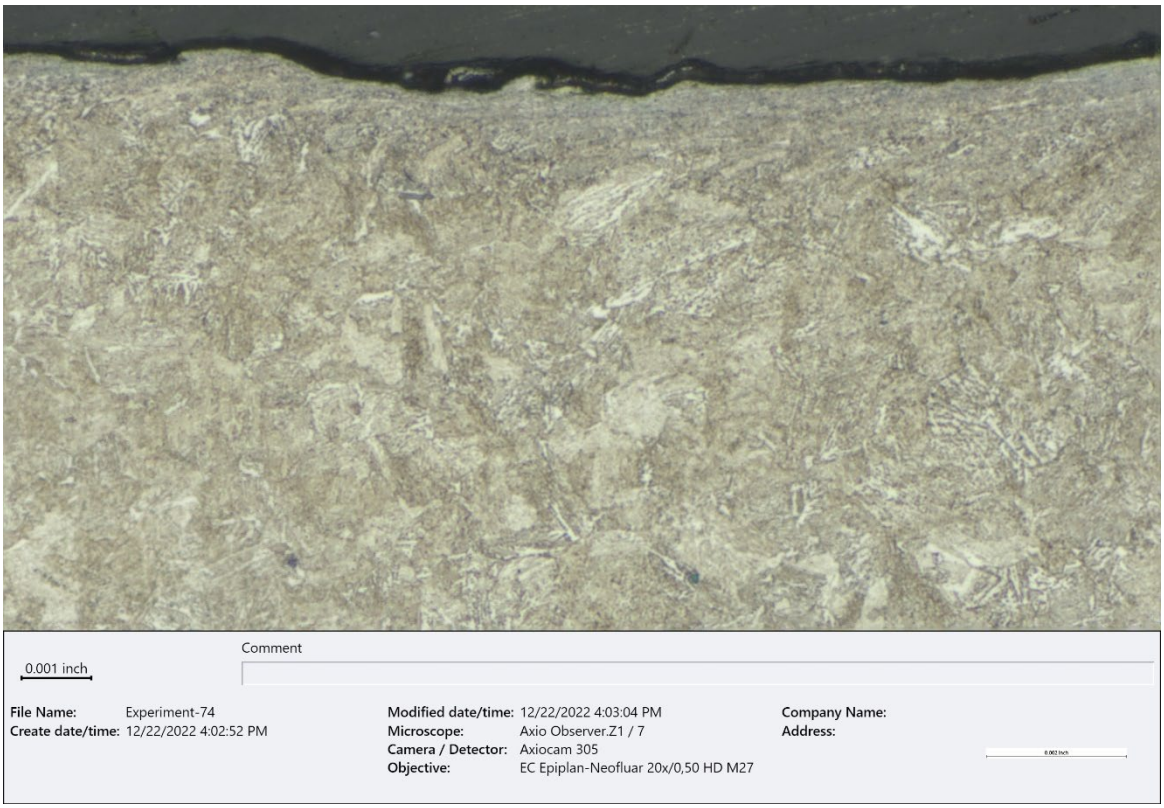

Figure 40. BF optical micrograph, etched to show grain deformation near the surface (~500X, etched 2% Nital).

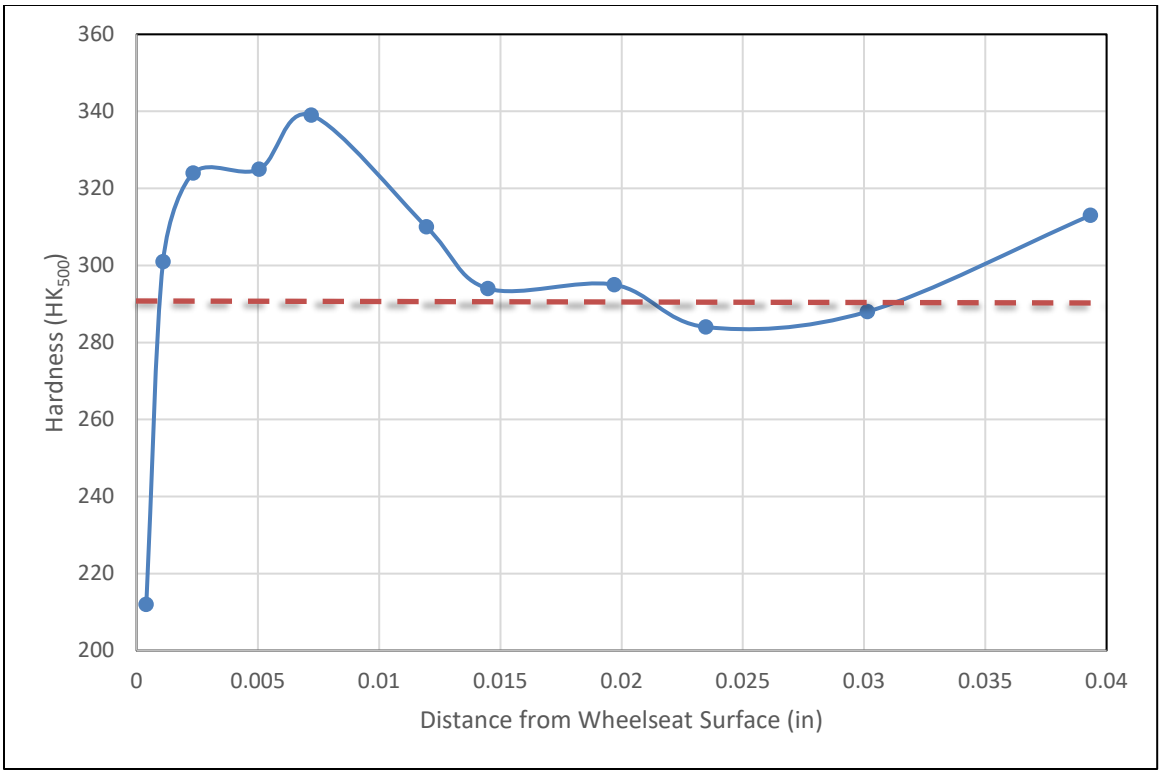

Figure 41. Chart of changes in microindentation hardness values from an area of the wheel seat surface of the axle shown in **Figure 39**. The orange dashed line represents the average microhardness of the axle, equivalent to 27 HRC.